ELSEVIER

Computers and Electronics in Agriculture
20 (1998) 117–130

Computers and electronics in agriculture

Defects segmentation on 'Golden Delicious' apples by using colour machine vision

V. Leemans *, H. Magein, M.-F. Destain

Faculté universitaire des Sciences agronomiques de Gembloux, Passage des déportés, 2, B-5030 Gembloux, Belgium

Received 18 August 1997; received in revised form 9 January 1998; accepted 16 January 1998

Abstract

A method based on colour information is proposed to detect defects on 'Golden Delicious' apples. In a first step, a colour model based on the variability of the normal colour is described. To segment the defects, each pixel of an apple image is compared with the model. If it matches the pixel, it is considered as belonging to healthy tissue, otherwise as a defect. Two other steps refine the segmentation, using either parameters computed on the whole fruit, or values computed locally. Some results are shown and discussed. The algorithm is able to segment a wide range of defects. © 1998 Elsevier Science B.V. All rights reserved.

Keywords: Computer vision; Colour vision; Image segmentation; Apple defects

1. Introduction

The European Community defines three quality categories for the fresh apples market (Journal of the European Community, 1989). The 'extra' class includes fruits with no defects or misshapenness. Good quality fruits presenting certain small defects (scab or russet for example) or a slight misshapenness are put in class I (or A in Belgium). In Class II (or B), more pronounced defects are tolerated. If the

* Corresponding author.

PII S0168-1699(98)00012-X

defect is too large or if the fruit pulp is strongly affected (like rot or insect holes), it is rejected as culls. These standards tolerate a small amount of misclassified fruits depending on the class and on the kind of defect. The general tolerance for the quality is 5% for class extra, and 10% for classes I and II. Belgian trade practices add four subclasses for Golden Delicious apples, following the ground colour of the fruit (noted as + + for the greenest, +, ' ' i.e. normal, and r for the yellows).

Apple quality grading, which implies the detection of the possible defects, their measurement (area or length) and their recognition, is actually done manually. Automation of this process could be done with machine vision and the first step is to detect or segment the defects. Some authors have studied this problem with monochrome cameras, while others have preferred to use colour cameras. Several approaches have been global, i.e. few parameters are computed to represent the whole image, while other approaches have been local and concern small areas.

Yang and Tillett (1994) and Yang (1994), quoting Rehkugler and Throop (1985), Davenel et al. (1988), present the situation for the monochrome approach. They link the mean grey level to the fruit colour, which varies locally. Because of the fruit curvature, the intensity decreases from the centre of the fruit to the boundaries. Furthermore, some noise exists due, amongst other things, to lenticels. The defects usually appear darker than the rest of the fruit, but the contrast between healthy and sick tissues changes from one defect to another. Mostly, their size and shape may vary strongly. For these reasons, simple techniques such as threshold or background subtraction give poor results, and pattern techniques are unusable. Yang finally declares that the global approach is best suited for large diffuse defects, while texture techniques are more convenient for spotty defects. Yang (1994) proposed the use of a 'flooding' algorithm to segment patch-like defects (russet patch, bruise, and also stalk or calyx area). This technique was improved by Yang and Marchant (1995) who applied a 'snake' algorithm to closely surround the defects. In both cases, noise had to be reduced, using median and Gaussian filters. Both algorithms produced small erroneous defects which could be eliminated by a threshold.

Using a colour camera, Heinemann et al. (1995) used the hue (H) to discriminate russet. It was a global approach, since the mean hue on the apple was computed. A discriminant function sorted the apple as accepted or rejected. The accuracy reached 82.5%, which is poor compared with European standards. Miller (1995) used HSI colour measurement for citrus sorting. The main idea was to compute mean differences and mean square differences with respect to a colour standard, for each colour parameter on the whole fruit. These values were normalised ((value − min)/(max − min)). A seventh parameter concerning the shape was added. Afterwards three different techniques were used (neural net, Bayesian–Gaussian separation and a non-parametric classifier) to sort the fruits as accepted or rejected. The maximum successful classifications reached 68.9–85.8%. The latter percentage is reached with the Bayesian method, depending on the citrus species. This method affords little discrimination between the kinds of defects and is probably too rough to grade apples with respect to the European standards, which require classification of the defect and determination of its dimensions.

Analysing the different techniques used to detect defects, it appears that with the monochrome approach the conditions impose sophisticated algorithms. This is due to the intensity variations from fruit to fruit and within a fruit from place to place, especially from the centre to the boundary. The first problem (differences between fruits) suggests either an algorithm using little a priori information, or information which does not depend on the fruit background colour, or a self-fitting algorithm. The second problem (differences in an image) inspires the use of a region-based algorithm. Of course, this also calls for lighting as suitable as possible. All these problems exist on colour images, but can be overcome by studying the different relations linking the three channels. An example is the lighting problem, where the ratio between two or more of the RGB channels or the H (hue) channel does not depend on the light intensity if the studied surface is mat and does not present any specular reflection. In most published research, those working with colour images either did not use the whole colour information (i.e. they selected one or two channels) or they computed a single parameter. Often, they did not segment the defect, but computed few general parameters representing the whole picture, losing the main part of the information related to space (i.e. the shape, local texture, etc.).

This paper presents a novel algorithm able to detect defects, using the whole significant colour information. This algorithm consists of three steps. The first is a coarse defect segmentation based on a statistical comparison between the colour of an individual pixel and the global colour of the fruit. The following ones, based either on a global or on a local approach, enhance the detection. They can be applied separately (the second or the third) or successively (the third following the second). These different configurations are evaluated.

2. Materials and methods

The image acquisition system included the following elements: a tunnel providing diffuse light, a colour camera, a frame grabber, and a personal computer (Pentium 133 MHz, 32 Mb RAM, two hard disks each having a 1 Gb capacity).

The tunnel was a horizontal cylindrical reflector (diameter 0.5 m, length 1.25 m). The inner surface was painted flat white and reflected the light provided by two 36 W fluorescent tubes (Philips model 33, colour temperature 4100 K) placed under the apple level. Two horizontal and one semicircular diffusers finished to distribute the light. The camera viewed the top of the fruit through a circular window on the upper part of the lighting chamber. A general diagram and a section diagram are presented in Fig. 1.

A 3-CCD matrix type camera (XC-003P, Sony) was placed at about 400 mm from the top of the fruit and was fitted with a 16 mm lens. The camera and a coupled frame grabber (Imascan Chroma, Imagraph) were able to acquire 720×540 pixels images, with a colour resolution of 3×8 bits per pixel.

The basic pretreatments were made using ImagePro software (Media Cybernetics), while other algorithms were developed in C++ (Visual C++, Microsoft).

2.1. Initial segmentation

This basic algorithm sorted each pixel belonging to the fruit image. It aimed to compare the pixel colour to a global colour of the fruit image. If the colour values were too different, i.e. higher than a threshold, the pixel was considered as defect. Otherwise it was classified as sound tissue.

Firstly the colour variability of defectless apples was studied. These fruits were chosen in class A. In order to cover a wide range of maturity, four sets of 20 apples belonging to each of the four ground-colour subclasses A+ +, A+, A and Ar were measured. The stem–calyx axis was placed perpendicular to the camera's optical axis. Four images of fruit cheeks were acquired at 90° rotation increments, around the stem–calyx axis. The first image was randomly chosen. The images were pretreated. First of all, a background correction eliminated the colour variations due to the data acquisition system (camera and frame grabber). This was made by using an image of a flat uniform white object (the background image). The colour of each pixel is replaced by the value of the expression:

$$\boldsymbol{NX} = \left[\frac{\boldsymbol{X} - \boldsymbol{mX}_{\mathrm{bl}}}{\boldsymbol{X}_{\mathrm{B}} - \boldsymbol{mX}_{\mathrm{bl}}} \times (\boldsymbol{mX}_{\mathrm{b}} - \boldsymbol{mX}_{\mathrm{bl}}) \right] + \boldsymbol{mX}_{\mathrm{bl}}$$

where $\boldsymbol{NX}$ is the RGB vector of the pixel, after correction; $\boldsymbol{X}$ is the RGB vector of the pixel, before correction; $\boldsymbol{mX}_{\mathrm{bl}}$ is the mean black level vector, i.e. the mean vector of an image acquired with the lens closed; $\boldsymbol{X}_{\mathrm{B}}$ is the colour vector of the pixel in the background image, at the same co-ordinate as $\boldsymbol{X}$; and $\boldsymbol{mX}_{\mathrm{B}}$ is the mean colour vector of the background image.

The resolution was divided in three linearly, which gave 240×180 pixels, 3.6 pix/mm^2. The image was also reframed. A 5×5 median filter was used to remove

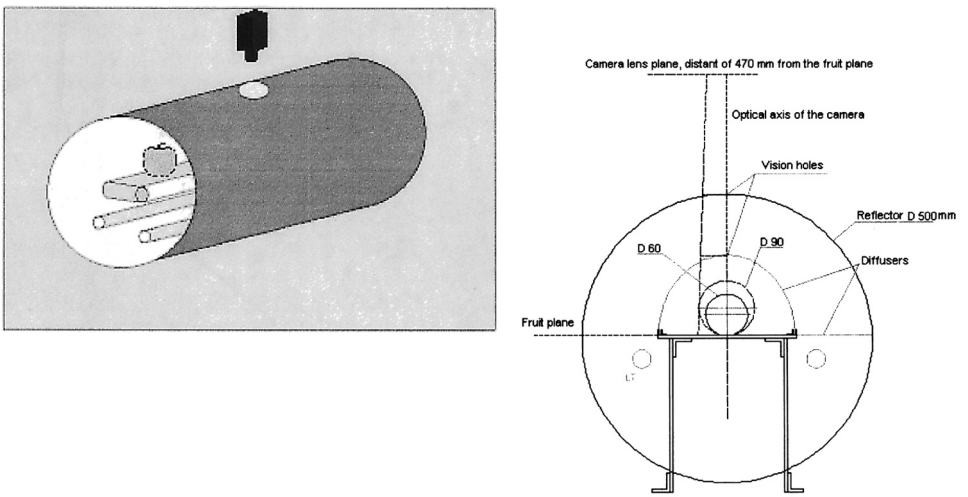

Fig. 1. General diagram (left, without the diffusers) and section (right) of the lighting chamber.

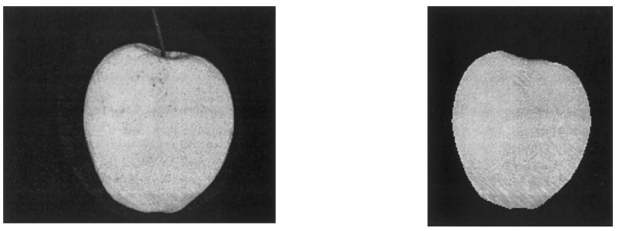

Fig. 2. Effect of the pretreatment: left, original image; right, final result.

the lenticels noise. Furthermore, the apple was eroded to suppress the darker area around the borders. To do this, the R channel was extracted; after a threshold operation at level 35, the bi-level image was eroded by four-neighbourhood kernel applied five times (Jähne, 1995); the result was converted to a RGB picture, and a logical bit AND operation with the 'median-filtered image' was applied to give the final result, shown in Fig. 2.

The colour model taken into account for a fruit image was a three-dimensional Gaussian distribution. It is based on the observation of several frequency distributions R, G and B, as shown in Fig. 3. Its mean vector may be expressed by:

$$\boldsymbol{m} = \begin{bmatrix} r \\ g \\ b \end{bmatrix}$$

where r, g and b correspond to the mean values of a fruit image for the three channels red, green and blue captured from the camera. The variance and covariance matrix was:

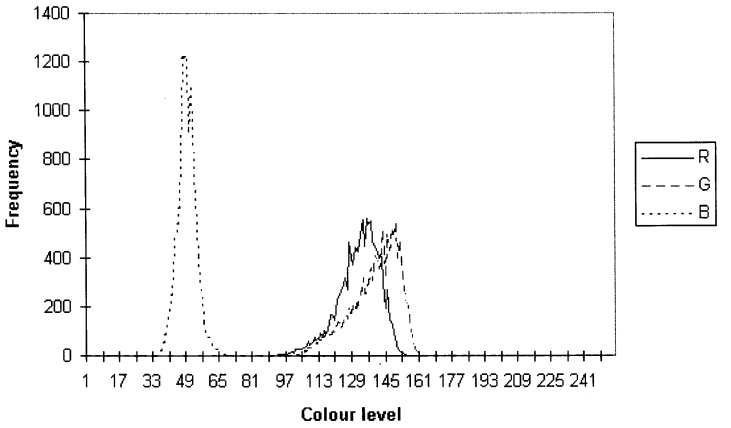

Fig. 3. Frequency distribution for R, G and B channels, for a Golden Delicious apple.

$$\Sigma = \begin{bmatrix} \sigma_{rr} & \sigma_{rg} & \sigma_{rb} \\ \sigma_{gr} & \sigma_{gg} & \sigma_{gb} \\ \sigma_{br} & \sigma_{bg} & \sigma_{bb} \end{bmatrix}$$

where σ_{rr}, σ_{gg} and σ_{bb} were the variances and σ_{rg}, σ_{gb} and σ_{rb} the covariances. It was found that the mean vector $\boldsymbol{m}$ varied from image to image, according to the fruit colour. On the other hand, one single variance and covariance matrix was considered for the whole population.

In a second step, apples affected by various defects were analysed. The colour of each pixel of an image was compared with the global colour of the image by using the Mahalanobis distance computed as follows:

$$\Delta^2 = (\boldsymbol{x} - \boldsymbol{m})' \Sigma^{-1} (\boldsymbol{x} - \boldsymbol{m}) \quad (1)$$

where Δ is the generalised distance; $\boldsymbol{x} = \begin{bmatrix} r_p \\ g_p \\ b_p \end{bmatrix}$ with r_p, g_p and b_p the measured values on each pixel, $\boldsymbol{m} = \begin{bmatrix} \tilde{r} \\ \tilde{g} \\ \tilde{b} \end{bmatrix}$ with $\tilde{r}$, $\tilde{g}$ and $\tilde{b}$ the median values on the images; $\Sigma^{-1}$is the inverse of the mean variance and covariance matrix, computed on the 80 healthy apples; and $(\boldsymbol{x} - \boldsymbol{m})'$ is the $(\boldsymbol{x} - \boldsymbol{m})$ vector transposed. The $\boldsymbol{m}$ vector is an estimation of the global colour of the fruit. Median values were used rather than mean values, since the former are less affected by the presence of a defect. If the square of the Mahalanobis distance, Δ^2 is high, the considered pixel is probably a defect. If Δ^2 is small, the pixel corresponds probably to healthy tissue. A threshold value D was chosen by analysing 32 apples affected by various defects (scab, russet, bruising, holes). The value of the threshold was a compromise between an over-segmentation for dark defects and an under-segmentation for light defects. In the rest of the paper, this part of the algorithm will be noted 'ID', with D the value of the threshold (for example I9).

2.2. Enhancing detection, global approach

In this second step, the medians' vectors and the average interquartile ranges were computed for the pixels belonging to healthy tissues and for those belonging to defective tissues, according to the initial segmentation. Afterwards, the 'distance' between each pixel and both medians is computed and weighed by the respective interquartile ranges. The pixel belongs to the closest class, the one for which the weighed distance is the smallest.

The weighed distances are given by:

$$D_{pd} = \frac{|r_p - \tilde{r}_d| + |g_p - \tilde{g}_d| + |b_p - \tilde{b}_d|}{Iqr_d} \quad (2)$$

$$D_{ph} = \frac{|r_p - \tilde{r}_h| + |g_p - \tilde{g}_h| + |b_p - \tilde{b}_h|}{Iqr_h} \quad (3)$$

where D_{pd} is the 'weighed distance' between the pixel and the defect class median; D_{ph} is the 'weighed distance' between the pixel and the healthy class median; r_p, g_p and b_p are the RGB pixel components; $\tilde{r}_d$, $\tilde{g}_d$ and $\tilde{b}_d$ are the RGB components of the median for the defects class; $\tilde{r}_h$, $\tilde{g}_h$ and $\tilde{b}_h$ are the RGB components of the median for the healthy class; and Iqr_d and Iqr_h are the average interquartile ranges for defects and healthy classes, respectively.

Some tests showed that there is no advantage in dividing each difference by the interquartile ranges of the considered channel. The mean value was thus used.

All the variables used in this part of the algorithm are computed on the image, and no parameter needed to be fitted. It will be noted 'II'.

2.3. Enhancing detection, local approach

The following lines explain how local information was taken into account. The algorithm worked like a filter combining the information belonging to the original image, and that coming from the segmented images.

A square area around the investigated pixel was considered (Fig. 3). Different sizes, 3×3, 5×5 and 7×7 were tested. Into this mask, the mean RGB vector for the healthy area and the same vector for the defect area were computed. The distances between the pixel under investigation and both means were computed:

$$D_{pd} = |r_p - \bar{r}_d| + |g_p - \bar{g}_d| + |b_p - \bar{b}_d| \quad (4)$$

$$D_{ph} = |r_p - \bar{r}_h| + |g_p - \bar{g}_h| + |b_p - \bar{b}_h| \quad (5)$$

D_{pd} is the 'distance' between the pixel and the defect class mean computed on the mask; D_{ph} is the 'distance' between the pixel and the healthy class mean computed on the mask; $\bar{r}_d$, $\bar{g}_d$ and $\bar{b}_d$ are the RGB components of the mean for the defects class; and $\bar{r}_h$, $\bar{g}_h$ and $\bar{b}_h$ are the RGB components of the mean for the healthy class.

The pixel was allocated to the nearest class. According to the possibly small number of pixels in one class, we did prefer the use of the mean instead of the median. We did not use any dispersion parameters, because they depend on local variations as well as on differences on wider areas. Therefore a global parameter is not convenient to describe the local variations. Computing them on the mask would not make sense because each class could contain only a few pixels, which does not represent the local variations. If the pixel belonged to the border of the fruit, the background pixels were not taken into account. This algorithm produces limited variations and had to be applied several times, to allow important corrections. The limitation is due to the size of the mask. If we consider a 5×5 mask (Fig. 4), a pixel at a distance greater than two pixels (according to the eight-neighbourhood rule) is not taken into account and could thus have any influence on the considered pixel. This means that the boundaries of a defect could only move by two pixels. The same set of 32 apples as before was used to determine the size of the mask and the number of repetitions. This algorithm will be noted III*s*,*n* where *s* is the size of the mask and *n* is the number of repetitions (for example: III5,3).

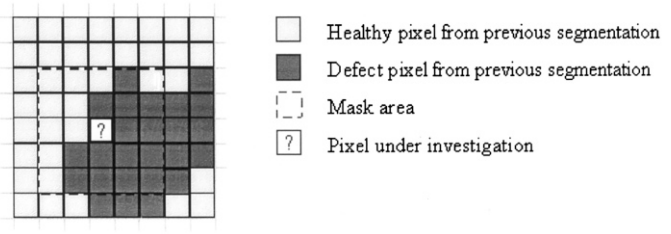

Fig. 4. Mask used by the algorithm.

2.4. Filtering

Unlike the model's fruit images, the images used to establish and control the algorithm may be filtered before or after the segmentation to eliminate small erroneous defects (lenticels etc.). The main defect must be preserved as much as possible, which requires a slight filtration. Before segmentation, two types of filters were tested: a '3×3 median filter' and a '3×3 box filter' as described by Jähne (1995). After segmentation, the image appeared in three levels. The background was in black, the defects in dark grey, and the healthy tissue was in white. A 'four-neighbourhood close filter' (Jähne, 1995) was tested (on images not filtered before segmentation). This morphological filter worked in two steps. Firstly the white areas are dilated, deleting the small dark holes. Secondly, the white areas are eroded, bringing back the main dark areas to their original size.

The border of the fruit was left as it stood.

3. Results and discussion

A set of 80 apples, including fruits of different qualities and damaged fruits, was used to test the different algorithm combinations. The defects encountered were bitter pit, fungi attack, growth defects, bruising, punches, insect holes, russeting and scab.

Four different algorithms combinations were tested, with one or three parameters to be fitted for each combination.

Some results are shown in Figs. 5–7; defect segmentation appear in the lower part of the figures. Four particular fruits were especially chosen to show the inherent difficulties due to the high variability encountered in apple sorting. The apple ground colours in images a, b, c and d were, respectively, typically ripe, green, yellow (over ripe) and very green (normal, +, r, ++ according to the Belgian ground colour classes). The first apple (Fig. 5a, Fig. 6a, Fig. 7a) had an old insect bite, which had produced a growth defect. At the left, the contrast between healthy and defective areas was clear, but on the right, the colour of the scar tissue tended gradually to the normal colour of the skin. The second defect (Fig. 5b, Fig. 6b, Fig. 7b) resulted from an early scab attack. The contrast was also clear;

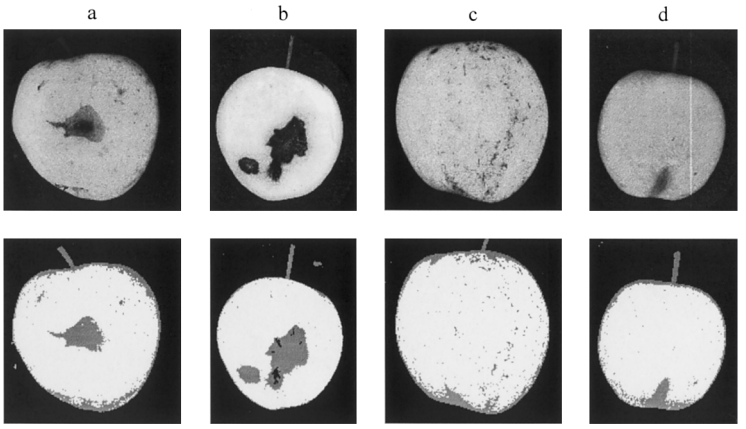

Fig. 5. Samples of apples with various defects, segmented with I9. a, Typical defect; b, well-contrasted defect; c, diffuse defect; and d, bruise.

however the middle of the defect was made of scar tissue and the defect presented a wide range of colours (dark to light brown, grey and green). The third defect (Fig. 5c, Fig. 6c, Fig. 7c) showed a diffuse russeting. Here, the contrast was low compared with the normal skin colour variations. The last defect (Fig. 5d, Fig. 6d, Fig. 7d) was a bruise. The healthy tissue was impaired, providing poor contrast, and the defect border was strongly blurred. No filtering was applied on the shown images. Fig. 5 concerns the initial segmentation with a threshold value equal to 9 (I9). Fig. 6 represents the enhancement using the global approach (I16 + II), while Fig. 7 shows the result of the three algorithms applied sequentially (I16 + II + III7,3).

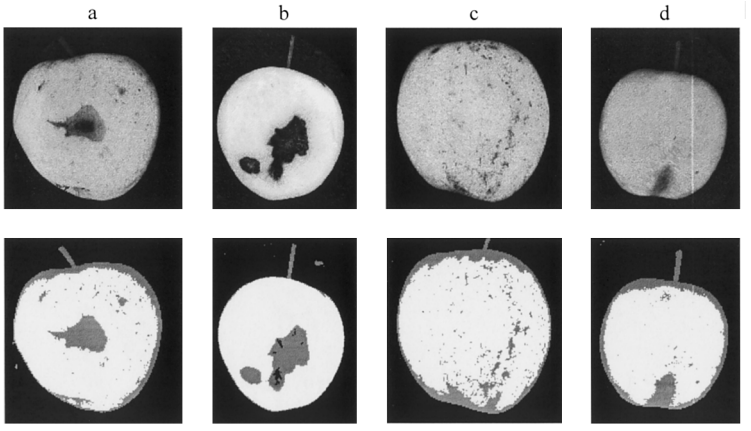

Fig. 6. Samples of apples with various defects segmented with I16 + II; a, Typical defect; b, well-contrasted defect; c, diffuse defect; and d, bruise.

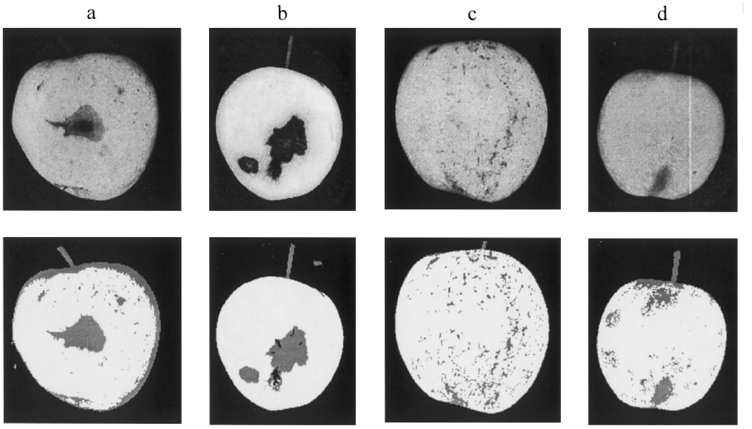

Fig. 7. Samples of apples with various defects segmented with I16 + II + III7,3. a, Typical defect; b, well-contrasted defect; c, diffuse defect; and d, bruise.

When the parameters of the different algorithms were near their optimum, the detection became accurate and the differences between the combinations were not easy to reveal. To give an appreciation of the results, three quotations were given for each image. The first one concerns the accuracy in defect segmentation, ranging from 0 to 5 (0 corresponds to no detection of an existing defect, 3 to a satisfactory detection, and 5 to a perfect detection). The second quote indicates how healthy tissue can be segmented as defect, also ranging from 0 to 5 (0 corresponds to a major area of good pixels falsely segmented, 3 to a few healthy pixels segmented as defect, and 5 to no good pixels segmented as defect). The last quote concerns the detection in the apple boundary area, ranging from 1 to 3 (1 corresponds to the whole apple border segmented as defect, 3 corresponds to a correct detection of the boundaries). The sum gives a global quotation. This evaluation was made by two operators, independently. Their results are naturally slightly different but the algorithms are sorted in the same order, which is the important point. It is possible to link these quotations to the kind of defects. Table 1 gives a summary of some of the quotations. The mean quotes are given for the two first results of the different algorithm combinations (three first for the last combination).

The initial segmentation algorithm was able to detect the defects as indicated by Fig. 5 and Table 1. Its ability to segment them was related to the contrast. It worked best with contrasted defects (Fig. 5-b), but was less accurate for other defects (Fig. 5-a, right part of the defect and Fig. 5-c). The border of the fruits was also slightly segmented as defect. However, this is not too important. When inspecting the fruit with a matrix camera, the area near the border is less explored than the central part. This problem would vanish in industrial processing. Indeed, rotation will be imposed to the fruits to see their entire surface, and lateral devices such as mirrors would be placed to see the sides of the apples. The best values were obtained with D around 9 or 16. The defects segmented with I16 present a slight

Table 1
Mean quotes for different algorithms combinations

	I9	I16	I9+II	I16+II	I16+ III7,3	I25+ III7,3	I9+II+ III7,3	I16+II+ III5,4	I16+II+ III7,3
Defect|defect	3.2	2.7	2.9	3.1	3.3	3.0	3.5	3.6	3.8
Healthy|healthy	3.7	3.6	3.3	3.7	3.2	3.7	3.0	3.5	3.7
Healthy boundary|healthy	1.8	2.4	1.1	1.5	2.8	3.0	2.1	2.2	2.3
Sum	8.7	8.7	7.3	8.3	9.3	9.7	8.6	9.4	9.8

Defect|defect quotes the accuracy in defect segmentation (0–5), healthy|healthy quotes how healthy tissue can be segmented as defect (0–5), and healthy boundary|healthy quotes the detection in the apple boundary area (0–3).

under segmentation, while I9 is more accurate. The detection improvement by the global approach was effective due to the algorithm which adapted the limit between accepted or rejected colours. For this reason it worked also on diffuse defects. The segmentation of the defect border in Fig. 6-a was correct, while the russeting (Fig. 6-c) and the bruising (Fig. 7-d) were detected, but not so accurately. For healthy fruits, presenting only some lenticels, the risk of erroneously segmented areas increased. Furthermore, if the stem or the calyx were present with light defects, the results were not quite satisfactory. The detection of the border as a defect increased, but as mentioned before, this problem is of no great importance. Combining the local approach enhancement on results of segmentation by I (I16 + III7,3 and I25 + III7,3) improved diffuse defect detection. Unfortunately, the number of good pixels segmented as defects also increased dramatically (Table 1). The enhancement shown by this combination on the sum was due to mainly to the enhancement in the border area. Finally, the three algorithms were applied sequentially. Three parameters had to be adjusted. The combination I16 + II + III7,3 was the best for the sum of the mean results and for the two first mean quotes (defects detection and healthy tissue segmentation Table 1). Its good segmentation efficiency appears in Fig. 7. In Fig. 7-a, the main defect is present as well as all the small, slightly contrasted blemishes. In Fig. 7-b, the border of the scab patch is very accurately segmented. The result in Fig. 7-c is far better. The main weakness of this algorithm is, for apples presenting defects close to the normal colour, like light russet or a bruise, to class in the defect some good pixels (Fig. 7-d). The previous step, the global enhancement, erroneously segmented some small areas. This was aggravated by the region's base enhancement because their colour was close to the normal colour of the neighbourhood. These pseudo-defects had a mean colour very close to the fruits' mean colour and often were lighter. They were thus easily recognised. A calyx end which is far greener than the rest of the fruit (which suggests a development problem) or a riper area were sometimes segmented as defect. The borders were clean, unless the apple presented marked ridges, producing a shaded border. It should also be noted that many of the lenticels were detected, even on healthy apples.

The segmentation revealed a lot of small spots. They could be removed using filtering or they could be ignored when counting the defects. Fig. 8 compares

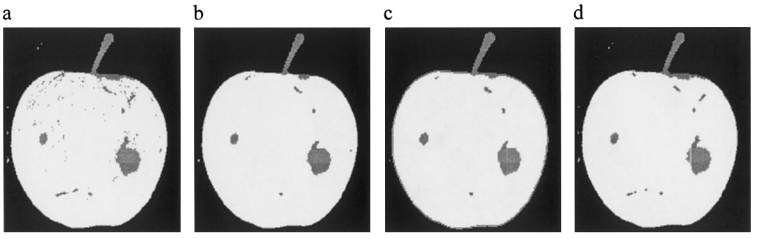

Fig. 8. Comparison of different filtering methods, applied on a segmented apple. a, No filtering; b, median filtering, before segmentation; c, median low pass filtering, before segmentation; and d, close filtering, applied on the result of the segmentation.

different filtering methods applied to an apple image before or after segmentation using the I16 + II + III7,3 algorithm. The different results are very close, but the last one (Fig. 8-d) seems most accurate, since it preserves slightly contrasted defects. The border of the defect is smoothed by filtration, which is advantageous for defect shape evaluation.

If we compare the different algorithms, the last solution (I16 + II + III7,3) was the most accurate, but the basic segmentation algorithm (I9) gave sufficient defect detection. The precision enhancement needs more computing time and is acceptable only if it is compatible with on-line application for a reasonable cost. The resolution has a major influence on the speed of the process, while the prefiltering is less important. The postfiltration concerns monochrome images, therefore it treats less information and is faster to compute.

4. Conclusions

An algorithm using colour information is presented to segment defects on Golden Delicious apples. It comprises three steps to detect both well-contrasted and diffuse defects. The basic step compares the colour of a pixel with that of a global model of healthy fruits by making use of the Mahalanobis distances. This algorithm gave satisfactory results with well-contrasted defects. A first enhancement was well suited for diffuse defects, but increased the part of healthy tissues segmented as defects, especially on the border and on healthy fruits. A second enhancement, consisting of a local approach, was able to correct these problems. The filtration of the segmented image is preferable to the filtration of the original image. The proposed algorithm was found effective in detecting various defects such as bruises, russet, scab, fungi or wounds.

Acknowledgements

This research is funded by the Federal Ministry of Agriculture of Belgium. Project no. D1/4-6121/5703 A

References

Davenel, A., Guizard, C.H., Labarre, T., Sevila, F., 1988. Automatic detection of surface defects on fruit by using a vision system. J. Agric. Eng. Res. 41, 1–9.

Heinemann, P.H., Varghese, Z.A., Morrow, C.T., Sommer, H.J. III, Crassweller, R.M., 1995. Machine vision inspection of Golden Delicious apples. Appl. Eng. Agric. ASAE 11 (6), 901–906.

Jähne, B., 1995. Digital Image Processing—Concepts, Algorithms and Scientifics Applications, 3rd ed. Springer-Verlag, New York.

Journal of the European Community, 1989. Norme de qualité des pommes et poires de table' règlement. CEE 920/89, no. L97/19, 11 April.

Miller, W.M., 1995. Optical defect analysis of Florida citrus. Appl. Eng. Agric. ASAE 11 (6), 855–860.

Rehkugler, G.E., Throop J.A., 1985. Apple sorting with machine vision. ASAE Paper 85-3543.
Yang, Q., Tillett, R.D., 1994. Apple surface feature for blemish detection. Proceedings of workshop COST 94–System and Operation for Post-harvest Quality, September 1993, Leuven, Belgium, pp. 93–107.
Yang, Q., 1994. An approach to apple surface feature detection by machine vision. Comput. Electron. Agric. 11, 249–264.
Yang, Q., Marchant, J.A., 1995. Accurate blemish detection with active contour models. Comput. Electron. Agric. 14, 77–89.